land

MDPI

Article

Bacterial Microbiota and Soil Fertility of *Crocus sativus* L. Rhizosphere in the Presence and Absence of *Fusarium* spp.

Beatrice Farda, Rihab Djebaili, Matteo Bernardi, Loretta Pace, Maddalena Del Gallo and Marika Pellegrini *

Department of Life, Health and Environmental Sciences, University of L'Aquila, Via Vetoio, 67100 Coppito, Italy
* Correspondence: marika.pellegrini@univaq.it; Tel.: +39-0862-433-258

Abstract: Intensive agricultural practices have led to intense soil degradation and soil fertility losses. Many soil-borne diseases affect these intensive agricultural soils, worsening the physical-chemical and fertility imbalances. Among the numerous pathogens, the genus *Fusarium* includes members that destroy many crops, including *Crocus sativus* L., which also impairs the composition and functions of the microbial communities. This work aimed to investigate, for the first time, the bacterial communities of the rhizosphere of saffron in the presence and absence of fusariosis. The rhizosphere of the saffron fields in the territory of L'Aquila (Italy) with and without fusariosis was sampled and subjected to a microbiological analysis. Culture-dependent methods characterized the fusariosis. The dehydrogenase activity assay was estimated. The metabarcoding of the *16S rRNA* gene, a metagenome functioning prediction, and a network analysis were also carried out. The results showed that fusariosis, when it is linked to intensive agricultural practices, causes alterations in the microbial communities of the rhizosphere. The culture-dependent and independent approaches have shown changes in the bacterial community in the presence of fusariosis, with functional and enzymatic imbalances. The samples showed a prevalence of uncultured and unknown taxa. Most of the known Amplicon Sequence Variants (ASVs) were associated with the Pseudomonadoa (syn. Proteobacteria) lineage. The composition and richness of this phylum were significantly altered by the presence of *Fusarium*. Moreover, pathogenesis appeared to improve the ASVs interconnections. The metagenome functions were also modified in the presence of fusariosis.

Keywords: saffron; fusariosis; soil microbial diversity; DHA assay; 16S metabarcoding; PICRUSt 2; rhizosphere

Citation: Farda, B.; Djebaili, R.; Bernardi, M.; Pace, L.; Del Gallo, M.; Pellegrini, M. Bacterial Microbiota and Soil Fertility of *Crocus sativus* L. Rhizosphere in the Presence and Absence of *Fusarium* spp. *Land* **2022**, *11*, 2048. https://doi.org/10.3390/land11112048

Academic Editors: Chiara Piccini and Rosa Francaviglia

Received: 8 October 2022
Accepted: 13 November 2022
Published: 15 November 2022

1. Introduction

The growing demand for healthy food from a growing human population requires intensive and efficient land management practices and crop control to reduce the disease losses [1]. However, intensive farming practices are leading to the degradation of agricultural soils and a gradual loss of their fertility [2]. Soil degradation leads, in turn, to the loss of its functions. Climate change also increases the uncertain and complex management of agricultural soil, jeopardizing its long-term viability, its biodiversity, and consequently, its functions. The use of chemical fertilizers is considered to be the fastest way to increase agricultural production. However, their cost and other constraints are increasingly discouraging farmers from using them [3]. These products also cause environmental pollution with negative consequences for human health [4].

A lack of knowledge about soil biodiversity has been identified as the main limitation to its management. The diversity of soil microbial communities can be critical for soil resilience to various abiotic and biotic stressors [5]. Microorganisms in agricultural soils have a significant impact on soil fertility, on the availability of nutrients for the plant and on the suppression of soil-borne plant diseases [6]. The conservation and sustainable use of soil microbial diversity are crucial for increasing agricultural productivity [7]. The loss of biodiversity has a detrimental impact of productivity, stability, and services [4]. According

to a recent meta-analysis, fields that undergo organic management practices had between 32% and 84% higher soil microbial biomasses (carbon, nitrogen, total phospholipid fatty acids) and enzymatic activities (dehydrogenase, urease, protease) than the conventional systems do. Crop rotation, legume intercropping, and organic inputs have all been linked to an increased microbial richness in agricultural soils [8,9].

The loss of soil biodiversity is also linked to the increase in soil-borne diseases, especially in agricultural ecosystems, resulting in higher production costs [6]. Among the numerous pathogens, the genus *Fusarium* includes members that cause diseases in many plants. *Fusarium* diseases are mainly associated with vascular wilt, but several species can cause the seedling wilt, crown, lower stem, root and seed rot, and head and seed plague [10]. *Fusarium* spp. live saprophytically on the roots, stems, leaves, flowers, and seeds of diseased and dead plants [11]. The fungus can survive on seeds (internal and external) or as spores or mycelium in the dead or infected tissues [12]. Within the *Fusarium* genus, *Fusarium oxysporum* is responsible for wilting of plants in nurseries and field crops, causing significant losses [11].

Saffron (*Crocus sativus* L.) is one of the valuable crops that is affected by *F. oxysporum.* Several fungal species belonging to *Fusarium*, *Rhizoctonia*, *Penicillium*, *Aspergillus*, *Sclerotium*, *Phoma*, *Stromatinia*, *Cochliobolus*, and *Rhizopus* genera affect saffron [13]. *Fusarium* corm rot, which is caused by *F. oxysporum*, is the most destructive disease [14]. Infected plants die early, thus reducing the corm yield, quality, and flower and stigma production [15]. *F. oxysporum* causes vascular wilt, as shown by yellowing of the leaf, the loss of turgidity, necrosis, wilting, and the plant's death.

A *Fusarium* infection occurs when the mycelium or germinating spores penetrate the plant's roots, enter the xylem, and produce microconidia. Vascular vessels become clogged by the accumulation of mycelium, spores, and the oxidation of the degradation products of enzymatic lysis. Toxins can cause vein clearing (the loss of chlorophyll production along the veins), a reduction in the photosynthesis rate, and tissue damage that leads to excessive water loss through transpiration [16]. Fusariosis also harms microbial communities' composition and functions. The recent study by Wang and collaborators highlighted the increase in the carbon cycle, the Calvin cycle, and the expression of hemicellulose and chitin degradation genes in watermelon soil in the presence of *Fusarium* [17].

The literature lacks studies which investigate the effect of *Fusarium* on the quality of the saffron rhizosphere. We hypothesized that *Fusarium* is closely associated with microbial biodiversity loss and a loss of the soil enzymatic activity. This work is aimed at investigating the bacterial communities of the saffron rhizosphere in the presence and absence of fusariosis. The rhizospheres of four saffron fields in the L'Aquila area (Italy) with different extensions of fusariosis were sampled. We performed the metabarcoding of *16s rRNA* and the dehydrogenase activity assay. The same analyses were also carried out on the rhizosphere of six saffron fields without fusariosis.

2. Materials and Methods

2.1. Soil Sampling

Ten saffron fields in the L'Aquila territory (Abruzzo region) were subjected to rhizosphere sampling at 20 cm depth in March 2021. Four fields showed evident fusariosis (ZF1, ZF2, ZF3, and ZF4) and six fields showed no evident pathogenesis (ZB1, ZB2, ZB3, ZB5, ZB6, and ZB7). Field ZF3 presented a less evident presence of the pathogen. Figure 1 shows an example of an evident fusariosis. Five soil sub-samples were collected per field following a non-systematic pattern. The soil samples were sieved (<2 mm) to remove large particles and plant debris. Fresh homogeneous aliquots of each soil sample were immediately processed for culturable approaches and enzymatic activity estimations. Ten aliquots of each soil sample were stored at −80° until they were processed for DNA extraction.

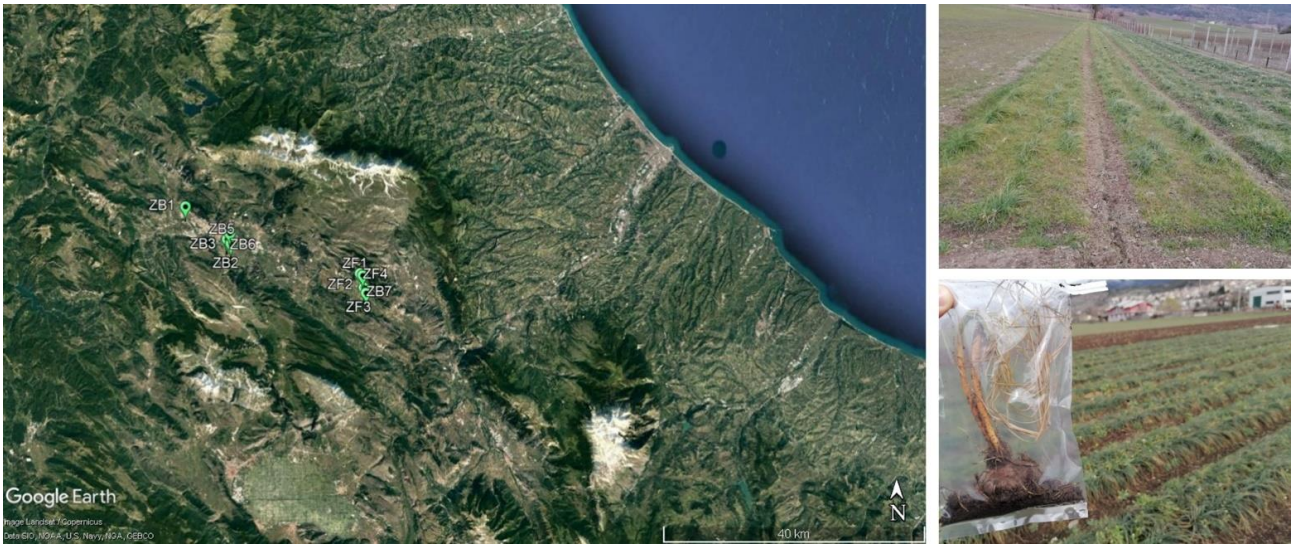

Figure 1. Geolocalization map of the sampling area and examples of a field and a corm with an evident *Fusarium* pathogenesis.

2.2. Fusariosis Pathogenesis Confirmation

The Fusarium pathogenesis was confirmed by the corms inspection and microbial culturable approaches. Three aliquots of each rhizosphere were processed in saline with 1% of Tween 20 (1:10 ratio) in a bag mixer for 30 min. After centrifugation at 4000 for 10 min, the supernatants were subjected to serial dilutions up to 1×10^{-7}. One hundred µL of each serial dilution were plated on Selective *Fusarium* Agar (SFA) [18] and incubated at 25 °C for five days. We confirmed the presence of Fusarium by macro- and microscopic observations of hyphae and spores and by spores sub-culturing on Potato Dextrose Agar PDA (Sigma-Aldrich, St. Louis, USA).

2.3. DNA Extraction and 16S rRNA Metabarcoding

The genomic DNA was extracted using 500 mg of homogenous samples according to the manufacturer's protocol (NucleoSpin®Soil, Macherey Nagel, Germany). The DNA content and purity were verified using a Nanodrop spectrophotometer (Thermo Scientific™, Waltham, MA, USA) and a Qubit fluorometer (Thermo Scientific™, Waltham, MA, USA). For each sample, the individual replicates were combined in an equimolar ratio. We performed paired-end *16S rRNA* community sequencing on the Mi-Seq Illumina technology (Bio-Fab Investigation, Rome, Italy), focusing on the V3 and V4 regions of the *16S rRNA* gene [19]. The filtering was performed, and the readings were evaluated for reliability, and they were counted. Using QIIME2 (qiime2-2020.2 version), the DADA2 plugin was used to build ASV (Amplicon Sequence Variant) [20]. The V3–V4 specific area was taken from the 16S file that was obtained from the SILVA database (https://www.arb-silva.de/ accessed on 14 October 2021) and used to train the classifier using the fit-classifier-naive-Bayes plugin.

2.4. Prediction of Metagenomic Functions

PICRUSt 2 (Phylogenetic Investigation of Communities by Reconstruction of Unobserved States) was used to predict the functional abundances based on *16S rRNA* gene sequencing data [21]. Pathways (PWYs), Enzyme on (EC) numbers and KEGG Orthologs (KOs) were predicted based on the Amplicon Sequence Variants (ASVs) sequence profiles/abundances (BIOM file format obtained from qiime2). PICRUSt 2 was run as a plugin of qiime2 with default parameters. We used the ALDEx2 (ANOVA-like differential expression) to perform the differential abundance testing between the two conditions with

1000 Monte Carlo samples and a One-way ANOVA test. An effect size that is greater than 1 was used as a significance cutoff with or without the BH correction of the raw *p* values.

2.5. Network Analysis

The network analyses were performed following Barberán et al. [22]. Briefly, the network was inferred by all of the possible Spearman rank correlation comparisons between the ASVs with more than 5 sequences (Spearman's correlation coefficient > 0.6 and statistically significant *p* value < 0.01). The networks were reconstructed with 90% identity ASVs as nodes and strong and significant correlations between the nodes as edges. The network topology was estimated by a metrics calculation (i.e., average node connectivity and path length, diameter, cumulative degree distribution, clustering coefficient, and modularity) [23]. All of the statistical analyses were performed in the R program using the Igraph [24] package. The networks were investigated and visualized using the interactive platform Cytoscape v 3.9.1 [25] and the Network analyzer v 4.4.8 tool [26].

2.6. Dehydrogenase Activity of Soil Samples

The soil dehydrogenase activity (DHA) was estimated using fresh soil samples [27]: Three aliquots of each soil sample (6 g) were placed in test tubes and mixed with 4 mL of distilled water. Each mixture was supplemented with 120 mg of $CaCO_3$ and 1 mL of 2,3,5-triphenyltetrazolium chloride (TTC 3% *v*/*w*) and incubated at 30 °C for 20 h. The samples were filtered, and triphenylformazane (TPF) was extracted using ethanol. The samples were then mixed and placed in the dark for 1 h. After incubation, the supernatant was recovered by centrifugation and analyzed at λ = 485 nm (Multiskan GO™—Thermo Scientific, Waltham, MA, USA). The results are expressed as μg TPF $g^{™1}$ $min^{™1}$ using a calibration curve (y = 0.0132x + 0.0083, R^2 = 0.999) [28].

2.7. Statistical Analysis

The data were analyzed by One-way Analysis of Variance (ANOVA) using the XLSTAT 2016 software (Addinsoft, Paris, France). Significant differences were calculated with Tukey's post hoc test at $p < 0.05$. The Primer 7 and PAST 4.03 software allowed the realization of the taxonomic bar plots of ASVs at the phylum (1%) and genus (1.5%) level and the calculation of alpha-diversity metrics (i.e., Simpson, Shannon, and Chao1 indices) of the different samples.

3. Results

3.1. Fusariosis Pathogenesis Confirmation

The presence of *Fusarium* spp. was confirmed by the microbiological approaches in all of the field where the pathogenesis was evident (ZF1-ZF4). Culturable fungal microflora that were developed on SFA showed a huge presence of *Fusarium.* Based on the morphology of the colonies that were observed, many species of *Fusarium* were present. Some of the isolates were allegedly identified as *Fusarium oxysporum* based on the shapes and sizes of the macro- and microconidia, the presence or absence of chlamydospores, the colony pigments, and the growth rates on PDA. No *Fusarium* isolates were observed from the fields where a pathogenesis was not evident.

3.2. DNA Extraction and 16S rRNA Metabarcoding

The *16S rRNA* gene metabarcoding results were used to investigate the diversity of the samples. As shown in Table 1, a high diversity was present both in the presence and absence of *Fusarium* (Shannon H values higher than 3.5). Sample ZB1 showed more taxa numbers (1454), individuals (36,299), and a high diversity index (Chao-1) when it was compared to the other field with fusariosis. Sample ZF3 presented the highest taxa values, individuals, and diversity indices.

Table 1. Diversity indices calculated on *16S rRNA* metabarcoding results using PAST 4.03 software. Soil samples were labelled as follows: ZB1–ZB7 labels refer to saffron soil samples without evident *Fusarium* pathogenesis; ZF1–ZF4 labels refer to saffron soil samples with *Fusarium* pathogenesis.

	ZB1	ZB2	ZB3	ZB5	ZB6	ZB7	ZF1	ZF2	ZF3	ZF4
Taxa_S	1454	1283	1141	1309	958	1345	1155	1270	2078	1440
Individuals (Richness ASVs level)	36,299	32,009	27,465	28,502	19,823	27,429	25,296	25,719	54,646	33,625
Shannon_H	6.657	6.538	6.41	6.594	6.281	6.657	6.501	6.587	6.994	6.761
Evenness_eˆH/S	0.5354	0.5385	0.5329	0.5583	0.5577	0.5788	0.5765	0.5711	0.5248	0.5996
Chao-1	1455	1285	1142	1310	958.7	1347	1156	1271	2080	1444

In the Table: ASVs, Amplicon Sequence Variants.

The *16S rRNA* metabarcoding results were also investigated for their structure and abundance. Figure 2 depicts the ASVs composition and abundances at the phylum level. Most of the ASVs were associated with Pseudomonadota (syn. Proteobacteria), which was followed by Actinobateriota. Latescibaterota and Entotheonellaeota were only present in ZB1 and ZB3, respectively. Firmicutes was only present in ZB2, ZB3, ZB6, and ZF2. Except for ZF1, Nitrospirota was absent in all of the ZF samples. Patescibacteria was not found in ZB3 and all of the ZF samples (except for ZF3). Except for ZB2, Planctomycetota was always present. The other phyla were shared by all of the samples.

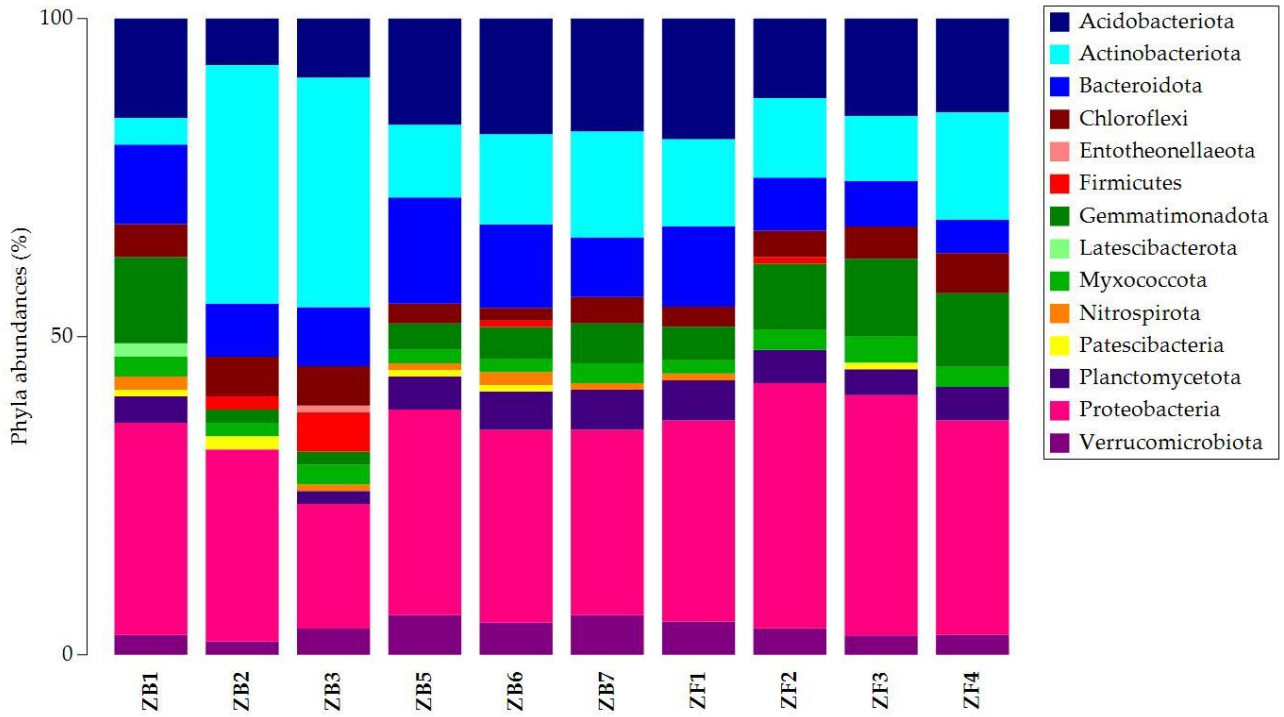

Figure 2. Taxonomic bar plot of the relative abundances of bacterial phyla associated with individual soil samples.

Given the relevance of the Pseudomonadota phylum within the bacterial communities in all of the fields, we carried out a comparison of the abundances and the composition of the ASVs based on the *Fusarium* presence/absence variable. Figure S1 shows the stacked boxplot of the comparison. In the presence of *Fusarium*, the abundances of the ASVs were lower than those that were observed in the absence of pathogenesis. This finding suggested a strong impact of the pathogenesis on richness of the ASVs associated with this phylum.

At the genus level, the common ASVs were those that were associated with uncultured and unknown taxa, which was followed by *Sphingomonas.* (Figure 3). *Vicinamibacteraceae*,

WD2101_soil_group, *RB41*, and *Rubrobacter* were also present in almost all of the samples. However, the occurrence of some genera was absent in the presence of *Fusarium* pathogenesis, i.e., *Streptomyces*, *Bacillus*, *Pseudomonas*, 67-14, *Nitrospira*, *Nocardioides*, *Adhaeribacter*, *Flavisolibacter*, *Flavobacterium*, *Gaiella*, KD4-96, MB-A2-108, *Stenotrophomonas*, *Terrimonas*, and UTCFX1. *Ellin6067* and *Massilia* were only present in the samples under the *Fusarium* pathogenesis condition.

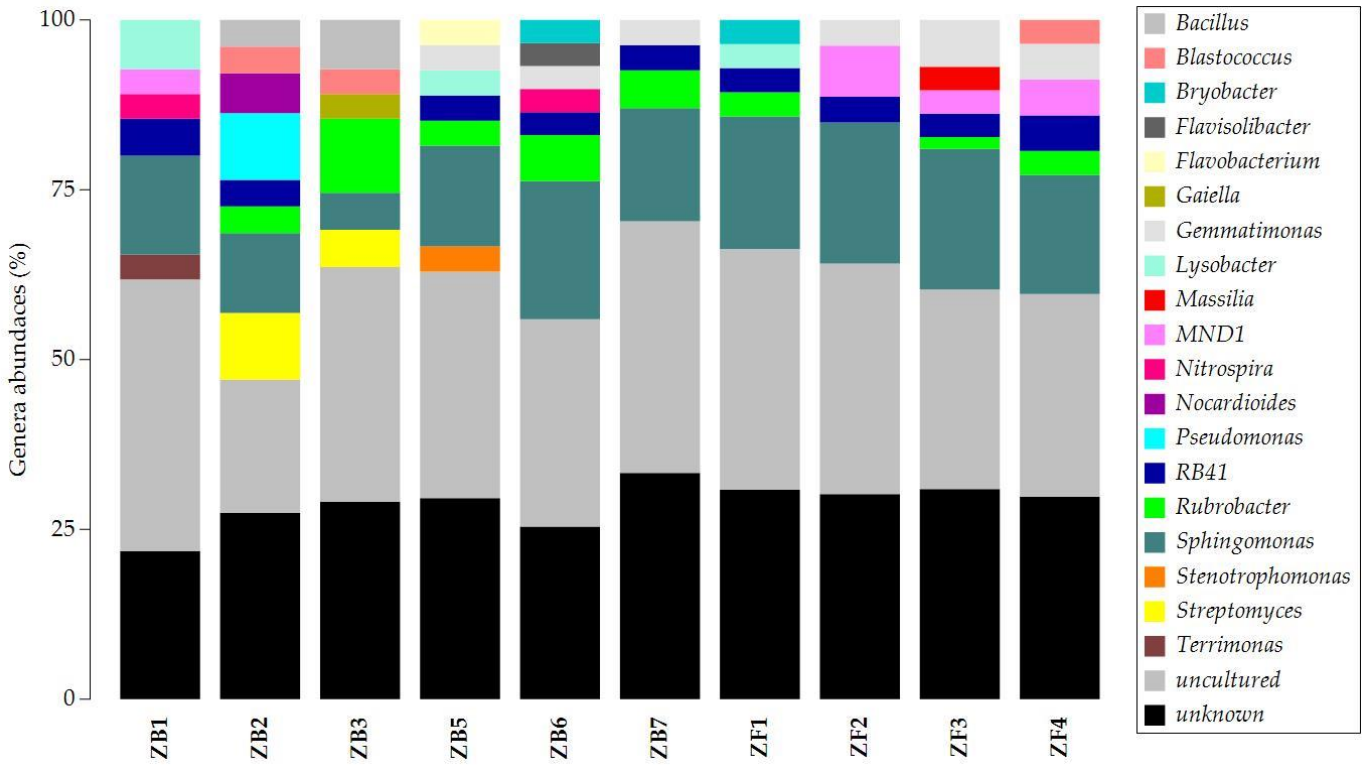

Figure 3. Taxonomic bar plot of the relative abundances of bacterial genera associated with individual soil samples.

3.3. Prediction of Metagenomic Functions

Some of the metabolic predictions showed differential abundances in the presence of fusariosis. Figures 4–6 show the Bland–Altman and Effect plots that shows the relationship between the effect size and the BH-adjusted *p* values (0.05 and 0.01) in the tests that were carried out for the ECs, KOs, and PWYs. Among the ECs (Figure S2), the most significant differences were observed for feature 1 (EC:1.1.1.21—aldose reductase) and 10 (EC 1.12.2.1—cytochrome-c3 hydrogenase), which were higher in the presence of *Fusarium*, and 11 (EC:1.3.1.87—3-(*cis*-5,6-dihydroxycyclohexa-1,3-dien-1-yl)propanoate dehydrogenase) and 61 (EC:4.3.1.29—D-glucosaminate-6-phosphate ammonia-lyase), which were higher in the absence of fusariosis.

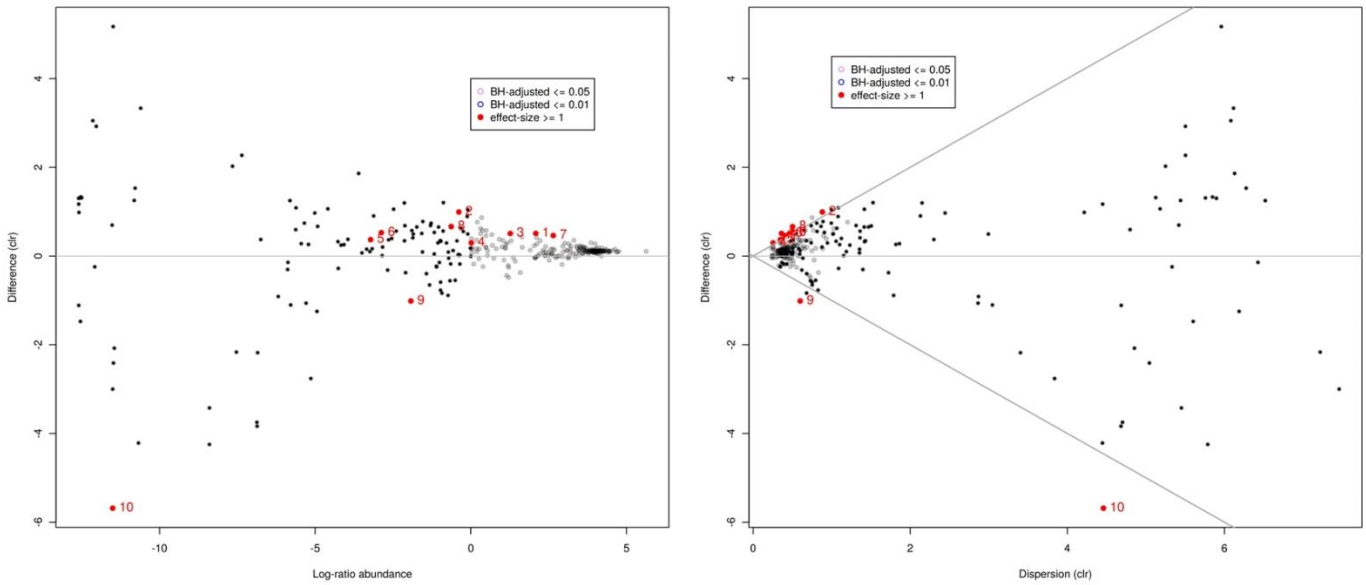

Figure 4. The panel on the left displays the Bland–Altman plot that shows the relationship between Abundance and Difference of the predicted pathways (PWYs) in the presence (lower part) and absence (upper part) of fusariosis. The panel on the right displays the Effect plot that shows the relationship between Difference and Dispersion of the PWYs between *Fusarium* and not *Fusarium* groups. In both of the plots, the 'not significant' features are shown in grey and black. Features that are statistically significant are in red.

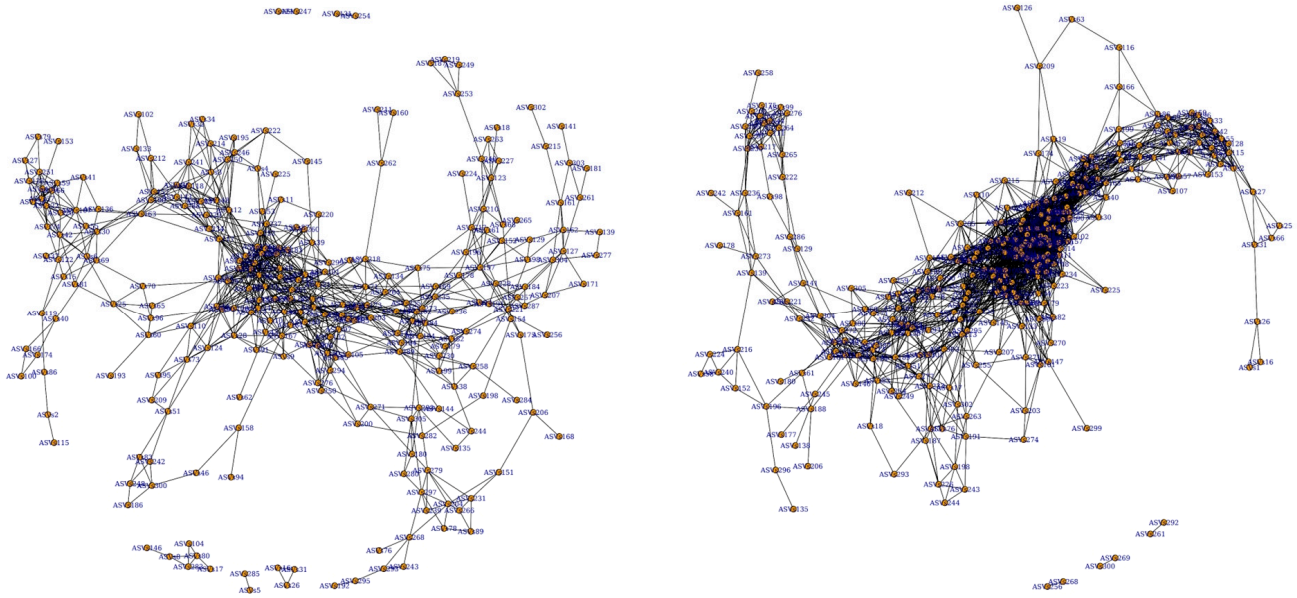

Figure 5. Network analyses carried out on saffron rhizosphere samples in the absence (on the **left**) and presence (on the **right**) of fusariosis. Jaccard similarity coefficient: 4.

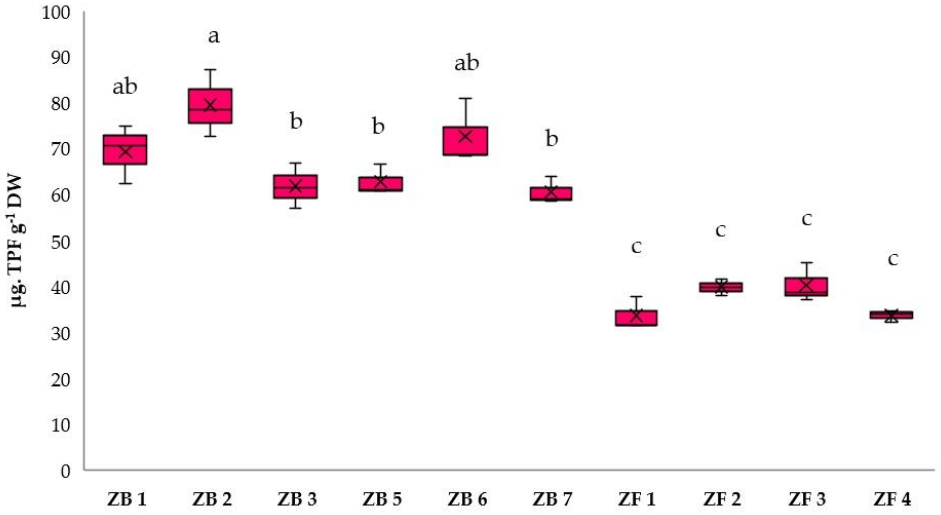

Figure 6. Dehydrogenase activity expressed as µg TPF g^{-1} DW. Results followed by the same case letter (a-c) are not significantly different according to Tukey's HSD post hoc test ($p > 0.05$).

Among the KOs (Figure S3), in the presence of *Fusarium,* higher counts were recorded for features 2 (K00011—aldehyde reductase), 24 (K02205—arginine/ornithine permease), 63 (K11601—manganese transport system substrate-binding protein), and 65 (K11638—two-component system, CitB family, response regulator CitT). In the absence of pathogenesis, the higher counts were recorded for the features 28 (K02791—maltose/glucose PTS system EIICB component), 32 (K03078—3-dehydro-L-gulonate-6-phosphate decarboxylase), and 35 (K03290—MFS transporter, SHS family, sialic acid transporter).

Among the PWYs (Figure 4), the features 9 (PWY-922—mevalonate pathway I) and 10 (THREOCAT-PWY—L-threonine metabolism) showed higher values in the presence of fusariosis. The pathogenesis altered the other PWYs, with low counts for features 1 (P124-PWY—fructose 6-phosphate pathway), 2 (P125-PWY—superpathway of (R,R)-butanediol biosynthesis), 3 (P161-PWY—acetylene degradation—anaerobic), 4 (PWY-5415—catechol degradation I), 5 (PWY-5529—superpathway of bacteriochlorophyll a biosynthesis), 6 (PWY-5531—3,8-divinyl-chlorophyllide a biosynthesis II—anaerobic), 7 (PWY-7254—TCA cycle VII—acetic acid-producers), and 8 (PWY-7315—dTDP-N-acetylthomosamine biosynthesis).

3.4. Network Analysis

The DNA sequencing results were also processed through a network analysis. Figure 5 shows the networks that were obtained for the soil samples with the presence and absence of Fusariosis. At a Jaccard similarity coefficient of four, the samples without *Fusarium* had a total number of 270 nodes and 989 edges, with an average number of neighbors of 7647. In the presence of pathogenesis, higher counts of all of the features were observed (295 nodes; 2750 edges; 19,010 average number of neighbors). A complete dataset of both groups was also processed, creating a network with the sample distribution base on the ASVs features. Figure S4 shows the interconnections among all of the samples based on shared ASVs occurrences, highlighting a close relationship among all of the samples.

3.5. Dehydrogenase (DHA) Activity

The results of the dehydrogenase activity analysis are presented in Figure 6. The samples without fusariosis showed the highest values of DHA ($p < 0.05$), with results of up to 79.43 µg TPF g^{-1} DW. Conversely, the samples with *Fusarium* pathogenesis recorded the lowest values ($p < 0.05$). No significant values among the fields with *Fusarium* pathogenesis were recorded ($p > 0.05$), with an average value of 36.84 µg TPF g^{-1} DW. Moreover, these samples presented the lowest values when they were compared to those from the field without the presence of *Fusarium*.

4. Discussion

The microbial diversity of the rhizosphere of numerous plants, including saffron, has been thoroughly studied using culture-dependent and -independent methodologies [29–32]. In this study, we investigated the changes that occur in the saffron rhizosphere in the presence of the *Fusarium* pathogenesis. The L'Aquila territory (Abruzzo, Italy) and the "*Zafferano dell'Aquila*" (a fine saffron variety with a protected designation of origin) were taken as a case study. Overall, the results suggest that pathogenesis does not affect the rhizosphere microbiota diversity and richness. However, the microbial communities' composition, structure, and functions were altered in the presence of the *Fusarium* pathogenesis.

A presence of uncultured and unknown taxa were found by the *16S rRNA* gene metabarcoding. Uncultured microorganisms are widespread in many environments. They play a crucial role in the biodegradation of various pollutants [33]. They constitute a buried group with a genetic resource encoding for unique valuable functions [34]. The uncultured microorganisms are detected in numerous degradation processes, allowing for efficient bioremediation by targeting specific eco-physiological niches [33]. The metagenomic analysis of chronically polluted coastal sediments revealed the presence of aromatic-ring-hydroxylating oxygenase, which is related to the biodegradation of polycyclic aromatic hydrocarbon as reported by Loviso et al. [35]. Likewise, the genus *Sphingomonas* is a part of the rhizospheric population, and it is linked with several biogeochemical cycles in soil and different metabolic processes [36].

In addition to the uncultured and unknown taxa, most of the ASVs were associated with Proteobacteria. In the presence of fusariosis, the abundances and taxa associated with this phylum were lower than they were in the healthy soils. Proteobacteria is one of the major phyla in soil ecosystems [37–40], with them having crucial roles in fixing the atmospheric nitrogen and mineralizing numerous soil nutrients [36]. This decrease in Proteobacteria is in line with the findings of Zhou et al., who described the same behavior for the banana rhizobacteria microbiota that were infected by *Fusarium* [41]. Proteobacteria have been closely associated with fungal pathogenesis in other plant species. Shen et al., for example, found that the prevalence of Proteobacteria is linked to the epidemic stage of wheat take-all disease [42]. In our case, this phylum is the most prevalent in the saffron rhizosphere, with it comprising up to 54% of the population [43].

At the genus level, the exclusive presence of *Bacillus*, *Nitrospira*, *Pseudomonas*, and *Streptomyces* in the healthy rhizospheres may indicate the presence of beneficial bacteria. These genera are usually associated with plant growth-promoting rhizobacteria (PGPR), with important biostimulant and biocontrol abilities [44–47]. Conversely, the exclusive presence of *Massilia* in the rhizospheres of samples with the pathogenesis indicates an unhealthy status. This lineage exploits the succession of communities within niches [48] and colonizes fungal hyphae with biocontrol effects [49]. A similar situation has been described by Bejarano-Bolívar et al., who described the presence of genera with biocontrol abilities (e.g., *Myxococcus* or *Lysobacter*) in the rhizosphere of an avocado that was affected by *Fusarium oxysporum* [50].

Metabolic predictions have highlighted interesting differences between the two groups. Among the most relevant, the increase in the mevalonate pathway I shows the increase in isoprenoids production. These compounds induce plant growth and development and improve the plant's response to environmental stresses [51]. The increase in the metabolic pathway of L-threonine indicates a high functionality of the community in the degradation of this amino acid [52]. These aspects suggest an attempt to counteract the pathogenesis by the microbial community of the rhizosphere.

Conversely, low counts of the other pathways related to the degradation of sugars, aromatic compounds, and hydrocarbons, the production of acetic acid and chlorophylls, and the production of sucrose metabolites were found. In line with previous reports, these decreases show less functionality in the presence of pathogenesis. The study by Wu et al., for example, described a higher carbohydrate and energy biosynthesis and

secondary metabolites in the *Panax notoginseng* rhizosphere in the presence of root-rot fungal pathogens [53].

The network analyses also confirmed the attempt to counter the pathogenesis by the rhizosphere microbial community. Pathogenesis appeared to improve the ASVs interconnections. As reported by the recent review by Siles et al. [54]. Conversely, in the presence of pathogenesis, the organic matter increases due to the plant's degradation. This organic supply can increase the saprotrophic and symbiotrophic interactions, producing a more interconnected network [54].

Estimating the soil enzymatic activity is another approach to studying soil microbial community alterations [55–58]. Among the soil enzymes, dehydrogenase converts hydrogen from an organic material to inorganic acceptors, oxidizing the soil organic substances [59,60]. Soil DHA is an early indicator of alterations in the biological activities of the soil [55]. In the presence of Fusariosis, we found a significant decrease in DHA, which is in line with the results of the literature. Low DHA values have been described for the tomato rhizosphere in the presence of fusariosis by Dukare et al. [61]. A negative correlation between the DHA and pathogenesis was also found in the tomato rhizosphere in the presence of *Ralstonia solanacearum* pathogenesis [62]. This finding confirms the lower metabolic functions of the saffron rhizosphere in the presence of fusariosis which is underlined by the prediction of metagenome functions.

5. Conclusions

In this study, we investigated changes in the saffron rhizosphere in the presence of *Fusarium* pathogenesis. The territory of L'Aquila (Abruzzo, Italy) and *Zafferano dell'Aquila* were taken as a case study. We found alterations in the microbial communities' composition, structure, and functions in the presence of the *Fusarium* pathogenesis. Conversely, the diversity and richness of the rhizosphere microbiota were not affected. A predominance of uncultured and unknown taxa was reported using *16S rRNA* gene metabarcoding, and most of the ASVs were attributed to Proteobacteria. Additionally, the taxa that are associated with this phylum were less abundant in the presence of fusariosis when they were compared to those in the healthy soil. A noteworthy presence of beneficial bacteria in the healthy rhizospheres and genera with biocontrol activity in the samples with the pathogen was signaled. The microbial taxa interconnections have also improved to face the pathogen attack. To our knowledge, this is the first study on the saffron rhizosphere. Therefore, our findings help to enrich the knowledge on the subject. These results can be used as a starting point for future investigation on the microbial taxa of the rhizosphere that are involved in the suppression of *Fusarium* wilt disease to be used as sustainable disease control agents. Intensive agricultural practices are the most common reasons for fusariosis. Intensive managements, that are associated with agrochemical use and mechanizations, unbalance the soil microbiota and lead to outbreaks of fungal pathogenesis. For this reason, future studies should also investigate the agricultural practices that are used in fields to highlight the possible variables that induce Fusariosis and to develop strategies to avoid or control *Fusarium* outbreaks early.

Supplementary Materials: The following supporting information can be downloaded at: https://www.mdpi.com/article/10.3390/land11112048/s1, Figure S1: Stacked bar plot that shows the comparison of the abundances of ASVs associated with Pseudomonadota (syn. Proteobacteria) phylum of the group with *Fusarium* pathogenesis (on the left) and without (on the right). In the bar plot, the main classes and orders of the phylum are shown. Figure S2: Comparisons of the enzymes (ECs) predicted in the presence (lower part) and absence (upper part) of fusariosis. The panel on the left displays the Bland–Altman plot that shows the relationship between Abundance and Difference of the ECs. The panel on the right displays the Effect plot that shows the relationship between Difference and Dispersion of the ECs. In both plots, the 'not significant' features are shown in grey and black. Features that are statistically significant are in red. Figure S3: Comparisons of the gene copies (KOs) predicted in the presence (lower part) and absence (upper part) of fusariosis. The panel on the left displays the Bland–Altman plot that shows the relationship between Abundance

and Difference of the KOs. The panel on the right displays the Effect plot that shows the relationship between Difference and Dispersion of the KOs. In both plots, the 'not significant' features are shown in grey and black. Features that are statistically significant are in red. Figure S4: Co-occurrence network analysis of sample carried out on the complete dataset of saffron rhizospheres with the absence and presence of fusariosis. Maximum Jaccard similarity coefficient.

Author Contributions: Conceptualization, M.P. and M.D.G.; methodology, L.P.; software, M.P.; validation, M.P. and M.D.G.; formal analysis, B.F. and M.B.; investigation, M.D.G. and M.P.; resources, L.P.; data curation, R.D. and B.F.; writing—original draft preparation, R.D., B.F., and M.B.; writing—review and editing, M.P. and M.D.G.; visualization, L.P.; supervision, R.D.; project administration, M.P.; funding acquisition, M.P. and M.D.G. All authors have read and agreed to the published version of the manuscript.

Funding: This research was funded by Regione Abruzzo, project reference: CUP: C19J21047230002 "Sviluppo di Protocolli Colturali per la Produzione di Zafferano Volti al Miglioramento dello Stato Fisiologico delle piante e alla Salvaguardia della Coltura Contro il Fungo Patogeno *Fusarium oxysporum*—PRO.ZAFF".

Institutional Review Board Statement: Not applicable.

Informed Consent Statement: Not applicable.

Data Availability Statement: The datasets generated and/or analyzed during the current study are available from the corresponding author on reasonable request.

Acknowledgments: We thank Luca Lepidi and Pio Feneziani, for the sampling's permissions and their availability, and Daniela Maria Spera for her professional support.

Conflicts of Interest: The authors declare no conflict of interest. The funders had no role in the design of the study, in the collection, analyses, or interpretation of data, in the writing of the manuscript, or in the decision to publish the results.

References

1. Hemathilake, D.M.K.S.; Gunathilake, D.M.C.C. Agricultural Productivity and Food Supply to Meet Increased Demands. In *Future Foods*; Elsevier: Amsterdam, The Netherlands, 2022; pp. 539–553.
2. Ambrosini, A.; de Souza, R.; Passaglia, L.M.P. Ecological Role of Bacterial Inoculants and Their Potential Impact on Soil Microbial Diversity. *Plant Soil* **2016**, *400*, 193–207. [CrossRef]
3. Aktar, W.; Sengupta, D.; Chowdhury, A. Impact of Pesticides Use in Agriculture: Their Benefits and Hazards. *Interdiscip. Toxicol.* **2009**, *2*, 1–12. [CrossRef] [PubMed]
4. Saleem, M.; Hu, J.; Jousset, A. More Than the Sum of Its Parts: Microbiome Biodiversity as a Driver of Plant Growth and Soil Health. *Annu. Rev. Ecol. Evol. Syst.* **2019**, *50*, 145–168. [CrossRef]
5. Dubey, A.; Malla, M.A.; Khan, F.; Chowdhary, K.; Yadav, S.; Kumar, A.; Sharma, S.; Khare, P.K.; Khan, M.L. Soil Microbiome: A Key Player for Conservation of Soil Health under Changing Climate. *Biodivers. Conserv.* **2019**, *28*, 2405–2429. [CrossRef]
6. Kennedy, A.C.; Smith, K.L. Soil Microbial Diversity and the Sustainability of Agricultural Soils. *Plant Soil* **1995**, *170*, 75–86. [CrossRef]
7. Rahobisoa, J.J.; Ratrimo, V.R.; Ranaivoarisoa, A. Mitigating Coastal Erosion in Fort Dauphin, Madagascar. In *Sustainable Living with Environmental Risks*; Springer Nature: Cham, Switzerland, 2014; Volume 9784431548, ISBN 9784431548041.
8. McDaniel, M.D.; Tiemann, L.K.; Grandy, A.S. Does Agricultural Crop Diversity Enhance Soil Microbial Biomass and Organic Matter Dynamics? A Meta-Analysis. *Ecol. Appl.* **2014**, *24*, 560–570. [CrossRef]
9. de Deyn, G.; Gattinger, A.; Lori, M.; Symnaczik, S.; Ma, P. Organic Farming Enhances Soil Microbial Abundance and Activity—A Meta-Analysis and Meta-Regression. *PLoS ONE* **2017**, *12*, e0180442.
10. Gwinn, K.D.; Hansen, Z.; Kelly, H.; Ownley, B.H. Diseases of Cannabis Sativa Caused by Diverse Fusarium Species. *Front. Agron.* **2022**, *3*, 796062. [CrossRef]
11. Summerell, B.A.; Botanic, R.; Sydney, G.; Wales, N.S.; Leslie, J.F. To Fusarium Identification. *Plant Dis.* **2003**, 117–128. [CrossRef]
12. Lei, S.; Wang, L.; Liu, L.; Hou, Y.; Xu, Y.; Liang, M.; Gao, J.; Li, Q.; Huang, S. Infection and Colonization of Pathogenic Fungus Fusarium Proliferatum in Rice Spikelet Rot Disease. *Rice Sci.* **2019**, *26*, 60–68. [CrossRef]
13. Sharma, K.D. Abel Piqueras Saffron (*Crocus sativus* L.) Tissue Culture: Micropropagation and Secondary Metabolite Production. *Funct. Plant Sci. Biotechnol. Saffron* **2010**, *4*, 64–73.
14. Mirghasempour, S.A.; Studholme, D.J.; Chen, W.; Zhu, W.; Mao, B. Molecular and Pathogenic Characterization of Fusarium Species Associated with Corm Rot Disease in Saffron from China. *J. Fungi* **2022**, *8*, 515. [CrossRef] [PubMed]
15. Palmero, D.; Rubio-Moraga, A.; Galvez-Patón, L.; Nogueras, J.; Abato, C.; Gómez-Gómez, L.; Ahrazem, O. Pathogenicity and Genetic Diversity of Fusarium Oxysporum Isolates from Corms of *Crocus sativus*. *Ind. Crops Prod.* **2014**, *61*, 186–192. [CrossRef]

16. Register, L.; Help, C. *Feasibility of Using Mycoherbicides for Controlling Illicit Drug Crops*; National Academies Press: Cambridge, MA, USA, 2011. [CrossRef]
17. Wang, T.; Hao, Y.; Zhu, M.; Yu, S.; Ran, W.; Xue, C.; Ling, N.; Shen, Q. Characterizing Differences in Microbial Community Composition and Function between Fusarium Wilt Diseased and Healthy Soils under Watermelon Cultivation. *Plant Soil* **2019**, *438*, 421–433. [CrossRef]
18. Leslie, J.F.; Summerell, B.A. *The Fusarium Laboratory Manual*, 1st ed.; Leslie, J.F., Summerell, B.A., Eds.; Blackwell Publishing Ltd.: Oxford, London, 2006; ISBN 9780813819198.
19. Mizrahi-Man, O.; Davenport, E.R.; Gilad, Y. Taxonomic Classification of Bacterial 16S RRNA Genes Using Short Sequencing Reads: Evaluation of Effective Study Designs. *PLoS ONE* **2013**, *8*, e53608. [CrossRef]
20. Bolyen, E.; Rideout, J.R.; Dillon, M.R.; Bokulich, N.A.; Abnet, C.C.; Al-Ghalith, G.A.; Alexander, H.; Alm, E.J.; Arumugam, M.; Asnicar, F.; et al. Reproducible, Interactive, Scalable and Extensible Microbiome Data Science Using QIIME 2. *Nat. Biotechnol.* **2019**, *37*, 852–857. [CrossRef]
21. Douglas, G.M.; Maffei, V.J.; Zaneveld, J.R.; Yurgel, S.N.; Brown, J.R.; Taylor, C.M.; Huttenhower, C.; Langille, M.G.I. PICRUSt2 for Prediction of Metagenome Functions. *Nat. Biotechnol.* **2020**, *38*, 685–688. [CrossRef]
22. Barberán, A.; Bates, S.T.; Casamayor, E.O.; Fierer, N. Using Network Analysis to Explore Co-Occurrence Patterns in Soil Microbial Communities. *ISME J.* **2012**, *6*, 343–351. [CrossRef]
23. Newman, M.E.J. The Structure and Function of Complex Networks. *SIAM Rev.* **2003**, *45*, 167–256. [CrossRef]
24. Csardi, G.; Nepusz, T. The Igraph Software Package for Complex Network Research. *InterJournal Complex Syst.* **2006**, *1695*, 1–9.
25. Shannon, P.; Markiel, A.; Ozier, O.; Baliga, N.S.; Wang, J.T.; Ramage, D.; Amin, N.; Schwikowski, B.; Ideker, T. Cytoscape: A Software Environment for Integrated Models of Biomolecular Interaction Networks. *Genome Res.* **2003**, *13*, 2498–2504. [CrossRef]
26. Assenov, Y.; Ramírez, F.; Schelhorn, S.-E.; Lengauer, T.; Albrecht, M. Computing Topological Parameters of Biological Networks. *Bioinformatics* **2008**, *24*, 282–284. [CrossRef] [PubMed]
27. Casida, L.E.J.R.; Klein, D.A.; Santoro, T. *Soil Enzymology, Soil Biology 22*; Springer: Berlin/Heidelberg, Germany, 1964; Volume 98.
28. Xie, J.; Hu, W.; Pei, H.; Dun, M.; Qi, F. Detection of Amount and Activity of Living Algae in Fresh Water by Dehydrogenase Activity (DHA). *Environ. Monit. Assess.* **2008**, *146*, 473–478. [CrossRef] [PubMed]
29. Ambardar, S.; Singh, H.R.; Gowda, M.; Vakhlu, J. Comparative Metagenomics Reveal Phylum Level Temporal and Spatial Changes in Mycobiome of Belowground Parts of *Crocus sativus*. *PLoS ONE* **2016**, *11*, e0163300. [CrossRef] [PubMed]
30. Ambardar, S.; Sangwan, N.; Manjula, A.; Rajendhran, J.; Gunasekaran, P.; Lal, R.; Vakhlu, J. Identification of Bacteria Associated with Underground Parts of *Crocus sativus* by 16S RRNA Gene Targeted Metagenomic Approach. *World J. Microbiol. Biotechnol.* **2014**, *30*, 2701–2709. [CrossRef] [PubMed]
31. Mahaffee, W.F.; Kloepper, J.W. Temporal Changes in the Bacterial Communities of Soil, Rhizosphere, and Endorhiza Associated with Field-Grown Cucumber (*Cucumis sativus* L.). *Microb Ecol* **1997**, *34*, 210–223. [CrossRef]
32. İnceoğlu, Ö.; Al-Soud, W.A.; Salles, J.F.; Semenov, A.V.; van Elsas, J.D. Comparative Analysis of Bacterial Communities in a Potato Field as Determined by Pyrosequencing. *PLoS ONE* **2011**, *6*, e23321. [CrossRef]
33. Rani, A.; Porwal, S.; Sharma, R.; Kapley, A.; Purohit, H.J.; Kalia, V.C. Assessment of Microbial Diversity in Effluent Treatment Plants by Culture Dependent and Culture Independent Approaches. *Bioresour. Technol.* **2008**, *99*, 7098–7107. [CrossRef]
34. Wang, Y.; Chen, Y.; Zhou, Q.; Huang, S.; Ning, K.; Xu, J.; Kalin, R.M.; Rolfe, S.; Huang, W.E. A Culture-Independent Approach to Unravel Uncultured Bacteria and Functional Genes in a Complex Microbial Community. *PLoS ONE* **2012**, *7*, e47530. [CrossRef]
35. Loviso, C.L.; Lozada, M.; Guibert, L.M.; Musumeci, M.A.; Sarango Cardenas, S.; Kuin, R.V.; Marcos, M.S.; Dionisi, H.M. Metagenomics Reveals the High Polycyclic Aromatic Hydrocarbon-Degradation Potential of Abundant Uncultured Bacteria from Chronically Polluted Subantarctic and Temperate Coastal Marine Environments. *J. Appl. Microbiol.* **2015**, *119*, 411–424. [CrossRef]
36. Agri, U.; Chaudhary, P.; Sharma, A.; Kukreti, B. Physiological Response of Maize Plants and Its Rhizospheric Microbiome under the Influence of Potential Bioinoculants and Nanochitosan. *Plant Soil* **2022**, *474*, 451–468. [CrossRef]
37. Deng, J.; Yin, Y.; Zhu, W.; Zhou, Y. Variations in Soil Bacterial Community Diversity and Structures Among Different Revegetation Types in the Baishilazi Nature Reserve. *Front. Microbiol.* **2018**, *9*, 2874. [CrossRef] [PubMed]
38. Yang, Y.; Viscarra Rossel, R.A.; Li, S.; Bissett, A.; Lee, J.; Shi, Z.; Behrens, T.; Court, L. Soil Bacterial Abundance and Diversity Better Explained and Predicted with Spectro-Transfer Functions. *Soil Biol. Biochem.* **2019**, *129*, 29–38. [CrossRef]
39. Zou, Z.; Yuan, K.; Ming, L.; Li, Z.; Yang, Y.; Yang, R.; Cheng, W.; Liu, H.; Jiang, J.; Luan, T.; et al. Changes in Alpine Soil Bacterial Communities With Altitude and Slopes at Mount Shergyla, Tibetan Plateau: Diversity, Structure, and Influencing Factors. *Front. Microbiol.* **2022**, *13*, 839499. [CrossRef] [PubMed]
40. Kim, H.-S.; Lee, S.-H.; Jo, H.Y.; Finneran, K.T.; Kwon, M.J. Diversity and Composition of Soil Acidobacteria and Proteobacteria Communities as a Bacterial Indicator of Past Land-Use Change from Forest to Farmland. *Sci. Total Environ.* **2021**, *797*, 148944. [CrossRef]
41. Zhou, D.; Jing, T.; Chen, Y.; Wang, F.; Qi, D.; Feng, R.; Xie, J.; Li, H. Deciphering Microbial Diversity Associated with Fusarium Wilt-Diseased and Disease-Free Banana Rhizosphere Soil. *BMC Microbiol.* **2019**, *19*, 161. [CrossRef]
42. Shen, Z.; Ruan, Y.; Chao, X.; Zhang, J.; Li, R.; Shen, Q. Rhizosphere Microbial Community Manipulated by 2 Years of Consecutive Biofertilizer Application Associated with Banana Fusarium Wilt Disease Suppression. *Biol. Fertil. Soils* **2015**, *51*, 553–562. [CrossRef]

43. Bhagat, N.; Sharma, S.; Ambardar, S.; Raj, S.; Trakroo, D.; Horacek, M.; Zouagui, R.; Sbabou, L.; Vakhlu, J. Microbiome Fingerprint as Biomarker for Geographical Origin and Heredity in *Crocus sativus*: A Feasibility Study. *Front. Sustain. Food Syst.* **2021**, *5*, 688393. [CrossRef]
44. Djebaili, R.; Pellegrini, M.; Bernardi, M.; Smati, M.; Kitouni, M.; del Gallo, M. Biocontrol Activity of Actinomycetes Strains against Fungal and Bacterial Pathogens of *Solanum lycopersicum* L. and *Daucus carota* L.: In Vitro and In Planta Antagonistic Activity. In Proceedings of the 1st International Electronic Conference on Plant Science, Online, 1–15 December 2020; MDPI: Basel, Switzerland, 2020; p. 27.
45. Wang, S.; Wang, J.; Zhou, Y.; Huang, Y.; Tang, X. Prospecting the Plant Growth–Promoting Activities of Endophytic Bacteria Franconibacter Sp. YSD YN2 Isolated from *Cyperus esculentus* L. Var. Sativus Leaves. *Ann. Microbiol.* **2022**, *72*, 1. [CrossRef]
46. Santoyo, G.; Orozco-Mosqueda, M.D.C.; Govindappa, M. Mechanisms of Biocontrol and Plant Growth-Promoting Activity in Soil Bacterial Species of Bacillus and Pseudomonas: A Review. *Biocontrol. Sci. Technol.* **2012**, *22*, 855–872. [CrossRef]
47. Donn, S.; Kirkegaard, J.A.; Perera, G.; Richardson, A.E.; Watt, M. Evolution of Bacterial Communities in the Wheat Crop Rhizosphere. *Environ. Microbiol.* **2015**, *17*, 610–621. [CrossRef] [PubMed]
48. Ofek, M.; Hadar, Y.; Minz, D. Ecology of Root Colonizing Massilia (Oxalobacteraceae). *PLoS ONE* **2012**, *7*, e40117. [CrossRef] [PubMed]
49. Raaijmakers, J.M.; Paulitz, T.C.; Steinberg, C.; Alabouvette, C.; Moënne-Loccoz, Y. The Rhizosphere: A Playground and Battlefield for Soilborne Pathogens and Beneficial Microorganisms. *Plant Soil* **2009**, *321*, 341–361. [CrossRef]
50. Bejarano-Bolívar, A.A.; Lamelas, A.; Aguirre von Wobeser, E.; Sánchez-Rangel, D.; Méndez-Bravo, A.; Eskalen, A.; Reverchon, F. Shifts in the Structure of Rhizosphere Bacterial Communities of Avocado after Fusarium Dieback. *Rhizosphere* **2021**, *18*, 100333. [CrossRef]
51. Venkateshwaran, M.; Jayaraman, D.; Chabaud, M.; Genre, A.; Balloon, A.J.; Maeda, J.; Forshey, K.; den Os, D.; Kwiecien, N.W.; Coon, J.J.; et al. A Role for the Mevalonate Pathway in Early Plant Symbiotic Signaling. *Proc. Natl. Acad. Sci. USA* **2015**, *112*, 9781–9786. [CrossRef]
52. Harris, J.A. Measurements of the Soil Microbial Community for Estimating the Success of Restoration. *Eur. J. Soil Sci.* **2003**, *54*, 801–808. [CrossRef]
53. Wu, Z.; Hao, Z.; Sun, Y.; Guo, L.; Huang, L.; Zeng, Y.; Wang, Y.; Yang, L.; Chen, B. Comparison on the Structure and Function of the Rhizosphere Microbial Community between Healthy and Root-Rot Panax Notoginseng. *Appl. Soil Ecol.* **2016**, *107*, 99–107. [CrossRef]
54. Siles, J.A.; García-Sánchez, M.; Gómez-Brandón, M. Studying Microbial Communities through Co-Occurrence Network Analyses during Processes of Waste Treatment and in Organically Amended Soils: A Review. *Microorganisms* **2021**, *9*, 1165. [CrossRef]
55. Campos, J.A.; Peco, J.D.; García-Noguero, E. Antigerminative Comparison between Naturally Occurring Naphthoquinones and Commercial Pesticides. Soil Dehydrogenase Activity Used as Bioindicator to Test Soil Toxicity. *Sci. Total Environ.* **2019**, *694*, 133672. [CrossRef]
56. Paz-Ferreiro, J.; Fu, S. Biological Indices for Soil Quality Evaluation: Perspectives and Limitations. *Land Degrad. Dev.* **2016**, *27*, 14–25. [CrossRef]
57. Aspray, T.; Gluszek, A.; Carvalho, D. Effect of Nitrogen Amendment on Respiration and Respiratory Quotient (RQ) in Three Hydrocarbon Contaminated Soils of Different Type. *Chemosphere* **2008**, *72*, 947–951. [CrossRef] [PubMed]
58. Dotaniya, M.L.; Aparna, K.; Dotaniya, C.K.; Singh, M.; Regar, K.L. Role of Soil Enzymes in Sustainable Crop Production. In *Enzymes in Food Biotechnology*; Elsevier: Amsterdam, The Netherlands, 2019; pp. 569–589.
59. Wolinska, A.; Stepniewsk, Z. Dehydrogenase Activity in the Soil Environment. In *Dehydrogenases*; InTech: London, UK, 2012.
60. Wiatrowska, K.; Komisarek, J.; Olejnik, J. Variations in Organic Carbon Content and Dehydrogenases Activity in Post-Agriculture Forest Soils: A Case Study in South-Western Pomerania. *Forests* **2021**, *12*, 459. [CrossRef]
61. Dukare, A.; Paul, S. Effect of Chitinolytic Biocontrol Bacterial Inoculation on Soil Microbiological Activities and Fusarium Population in Rhizophere of Pigeon Pea (*Cajanus cajan*). *Ann. Plant Prot. Sci.* **2018**, *26*, 98. [CrossRef]
62. Posas, M.B.; Toyota, K.; Islam, T.M. Inhibition of Bacterial Wilt of Tomato Caused by Ralstonia Solanacearum by Sugars and Amino Acids. *Microbes Environ.* **2007**, *22*, 290–296. [CrossRef]